Pergamon

PII: S0042-6989(96)00281-7

Vision Res., Vol. 37, No. 22, pp. 3145–3161, 1997

Printed in Great Britain
0042-6989/97 $17.00 + 0.00

Contour Integration in Strabismic Amblyopia: the Sufficiency of an Explanation Based on Positional Uncertainty

ROBERT F. HESS,*† WILLIAM McILHAGGA,* DAVID J. FIELD*

Received 9 April 1996; in revised form 13 August 1996

Contour integration was measured in a group of strabismic amblyopes to determine if an explanation based solely on positional uncertainty was sufficient to explain performance. The task involved the detection of paths composed of micropatterns with correlated carrier orientations embedded in a field of similar micropatterns of random position and orientation (Field *et al.* Contour integration by the human visual system; Evidence for a local "association field". *Vision Research, 33*, 173–193, 1993). The *intrinsic positional uncertainty* for each amblyopic eye was measured with the same stimulus and it was found that in 10 out of our 11 amblyopic subjects, the reduced performance of the amblyopic eye could be modelled by the normal eye with an equivalent amount of positional uncertainty added to the stimulus. We conclude that the rules by which cellular outputs are combined, at least as reflected by this task, are normal in amblyopia. © 1997 Elsevier Science Ltd

Amblyopia Association Positional uncertainty Contour integration

INTRODUCTION

Our understanding of the nature of the processing deficit in amblyopia is still in its infancy. Neurophysiological models have suggested that apart from an elevated contrast threshold in neurons tuned to high spatial frequencies, the number and properties (Singer *et al.*, 1980; Mower *et al.*, 1982; Chino *et al.*, 1983; Freeman & Tsumoto, 1983; Crewther & Crewther, 1990; Blakemore & Vital-Durand, 1992) of individual neurons receiving input from the strabismic eye are normal. Psychophysical investigations have highlighted two perceptual deficits. First, contrast sensitivity is reduced especially at high spatial frequencies and second, positional accuracy is impaired for targets both at the acuity limit (Levi & Klein, 1982, 1985, 1990) and for targets of all sizes (Hess & Holliday, 1992; Demanins & Hess, 1996).

Although there is good agreement between the neurophysiological studies on animals and the psychophysical studies in humans concerning the contrast sensitivity deficit, there is as yet no neurophysiological correlate of the positional deficit revealed by psychophysics. The fact that the neurophysiology suggests that there is not a significant difference in the number of cells driven by the amblyopic eye in strabismic animals goes against any simple explanation based on undersampling (Levi & Klein, 1986). Additional psychophysical evidence against an undersampling notion comes from two recent studies. In the first, it was shown that, contrary to the prediction of an undersampling model, there was no correlated *suprathreshold* contrast discrimination deficit (Hess & Field, 1994). In the second, using a direction discrimination task (Hess & Anderson, 1993), no evidence of spatial aliasing was observed within the central field of severely amblyopic individuals. An alternate hypothesis, the "Neural Disarray Hypothesis" was proposed (Hess *et al.*, 1978; Hess, 1982; Hess *et al.*, 1990; Hess & Field, 1994) in which the spatial inaccuracy is the result of mis-wired cells rather than fewer cells. It was proposed that there was a loss of fidelity in the functional topology in V1 due to a disruption of the normal processes that maintain this in calibration (Hess & Field, 1994).

Here we examine whether these two deficits are a sufficient explanation of the perceptual deficit in amblyopia. To answer this we use a task which we have recently developed which may bear on how the outputs of neurons from different orientation columns in V1 are combined to detect contours. This allows us to assess whether the rules of association are normal in amblyopia and whether any anomalies exist more central to the site of the proposed neural disarray.

Our results suggest that in the majority of strabismic amblyopes contrast sensitivity and positional uncertainty are sufficient to explain the amblyopic deficit. The rules

*McGill Vision Research Unit, Department of Ophthalmology, McGill University, Montreal, Quebec, Canada.
†To whom all correspondence should be addressed.

by which the outputs of cells with different preferred orientations are combined to define contours using this particular task appear to be normal in amblyopia. However, strabismic amblyopes are by no means a homogeneous group. We found one out of our group of 11 amblyopes whose results did suggest that there was a residual anomaly more central to the site of the positional uncertainty.

METHODS

In all experiments the observers' task was to identify which of two presentations contained the "path stimulus". A path stimulus consisted of a set of oriented Gabor elements aligned along a common contour, embedded in a background of similar, but randomly oriented Gabor elements. A no-path stimulus consisted of just randomly placed and randomly oriented Gabor elements. Gabor elements were used to control the spatial frequency composition of the stimuli so that the path could not be extracted by a single broad band detector. By using such stimuli we hope to gain a better understanding of the combinatorial rules which govern the outputs of visual neurons used in the extraction of the path from the background elements.

Stimuli.

Oriented spatial frequency bandpass elements were used in this study; the oriented Gabor elements were defined by the equation:

$$g(x, y, \theta) = c\sin(2\pi f(x\sin\theta + y\cos\theta)\exp\left(\frac{-x^2 + y^2}{2\sigma^2}\right) \quad (1)$$

where θ is the element orientation, from 0 to 360 deg, (x, y) is the distance in degrees from the element centre, and c is the contrast. The sinusoidal frequency $f = 0.05$ c/pixel, the space constant $\sigma = 0.4 \times \lambda$. The contrast was

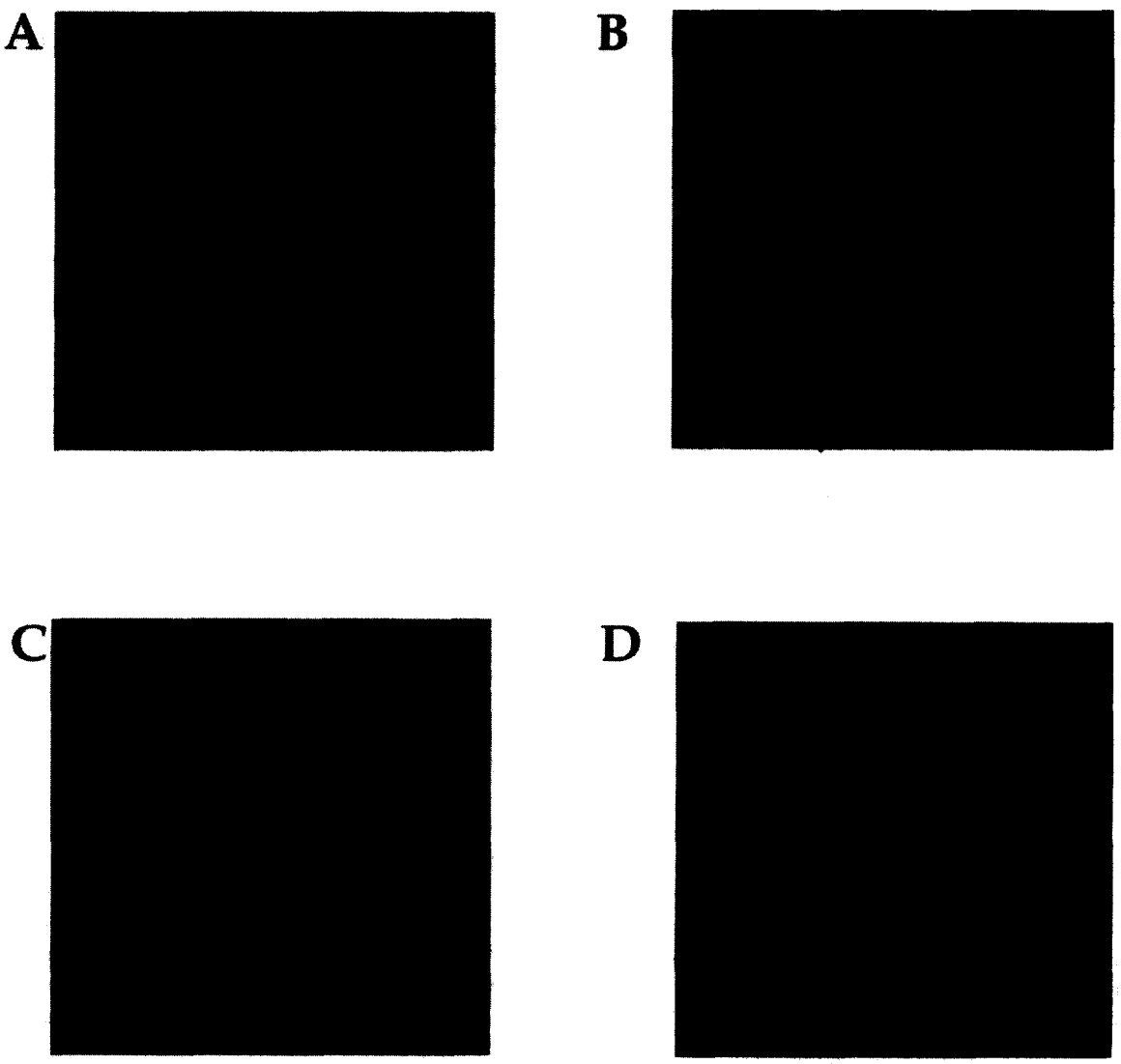

FIGURE 1. A path comprising eight micropatterns (end points indicated by arrows) is embedded in a field of randomly oriented micropatterns of the same form. Paths are shown for different path angles (see Fig. 2); (A) 0 deg, (B) 10 deg, (C) 20 deg and (D) 30 deg.

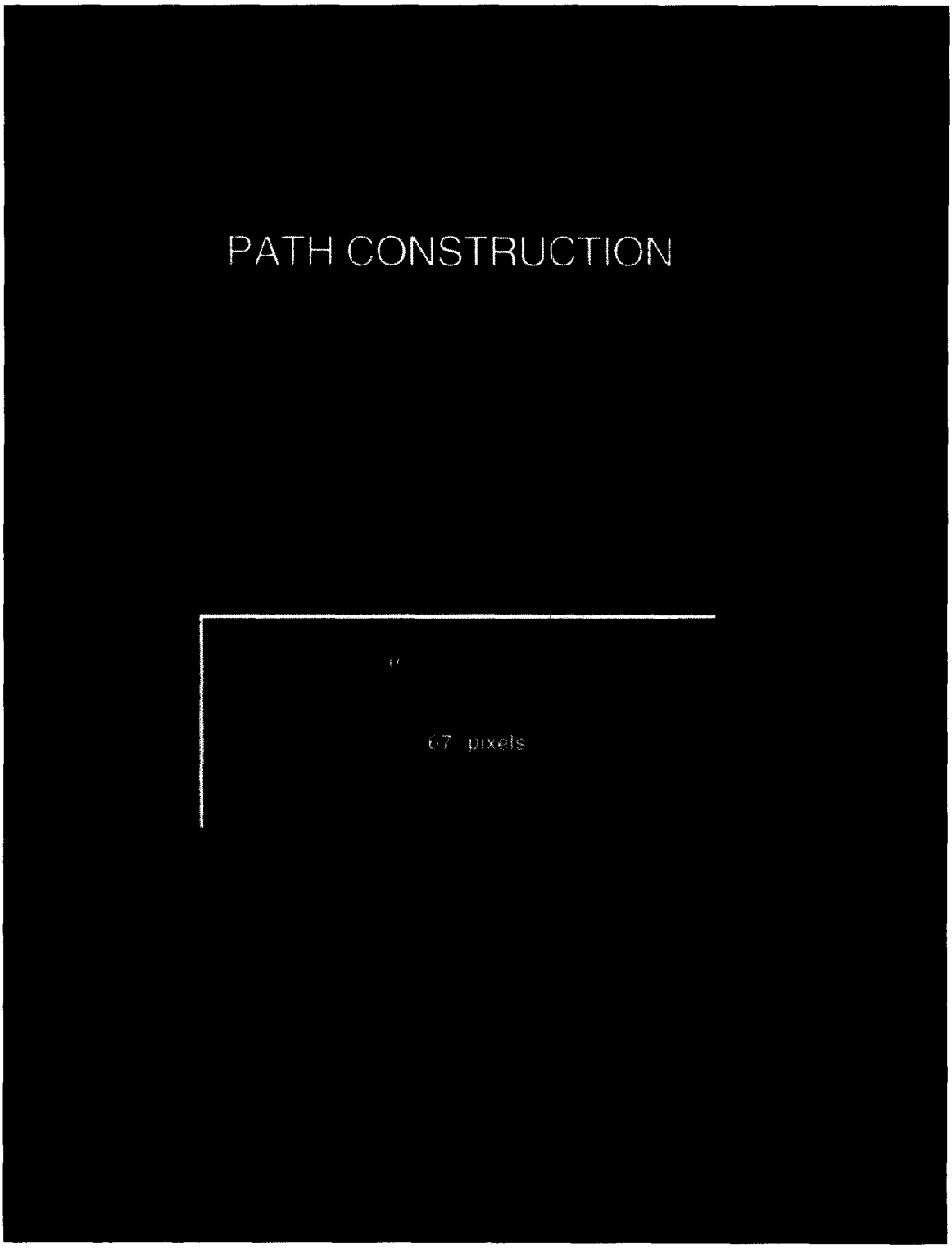

FIGURE 2. Path construction. Angle α is the path angle and since in this example the elements are perfectly aligned with the path, the element angle is zero.

90%. The spatial frequency varied for the particular amblyope (ranged from 3 to 12 c/deg).

A no-path stimulus was constructed in the following way. A 624 pixel wide square was divided into a 13×13 grid of equally sized cells. A Gabor element of random orientation was placed randomly in each display cell, with the restriction that each cell contain the centre of only one Gabor element. This eliminates the clumping of elements due to random placement. The elements were also placed to avoid overlap as much as possible. An empty cell occurred if the cells' Gabor patch could not be placed without significantly overlapping any of it's neighbours (i.e. crowded out by it's neighbours). There were fewer than four per image.

A path stimulus consisted of two parts; the path itself and the background (Fig. 1). The construction of the path

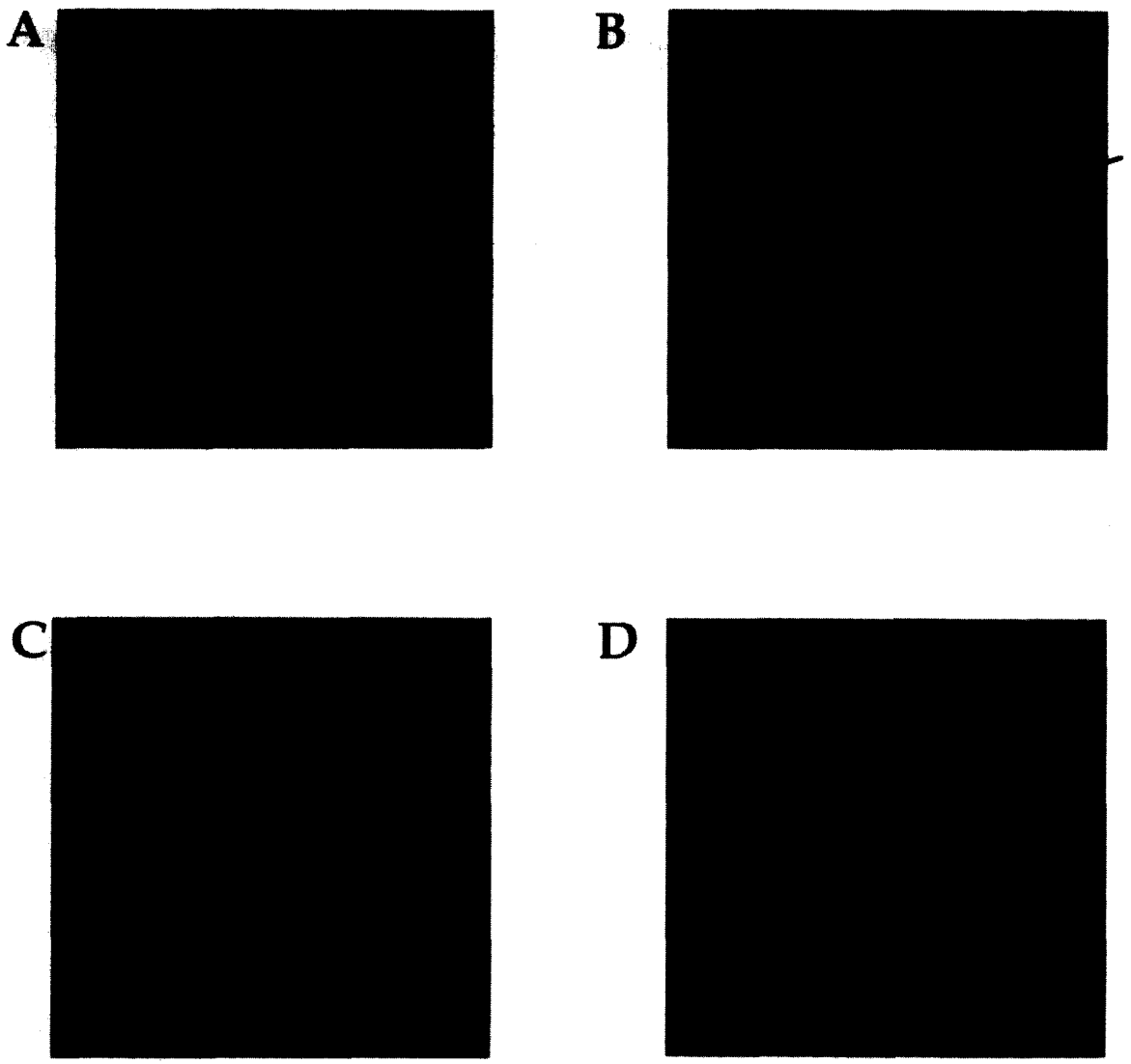

FIGURE 3. Examples of paths all of zero path angle with varying amounts of Gaussian distributed jitter added to the path element angle [(A) $\sigma = 0$ deg; (B) $\sigma = 10$ deg; (C) $\sigma = 20$ deg; (D) $\sigma = 30$ deg].

is illustrated in Fig. 2. The path had a backbone of 8 invisible line segments; each line segment was of length 67 pixels and the line segments joined at an angle uniformly distributed from $\alpha - 4$ to $\alpha + 4$ deg. α is called the *path angle*. Gabor elements were then placed at the middle of each line segment. The orientation θ of each element was the same as the orientation of the line segment on which it was placed. The *element angle* which is defined as the angle that the oriented element makes with the invisible backbone would be zero in this case. In some experiments (Fig. 3 for demonstration and Fig. 9 for data), the element angle was determined by a random variable. The orientation of each line segment was ambiguous (within the range 0–360), but traversing the path from one end to the other imposes a direction (and hence an unambiguous orientation) on each of the component line segments. Finally to avoid random changes in path detection due to random path closure which can have significant effects on path detection (Kovacs & Julesz, 1993), the path was checked to ensure that it neither intersected itself, nor looped back on itself. If so it was discarded and a new path generated.

The entire path contour was pasted into the display at a random location, ensuring the centres of the Gabor elements occupied different cells. Finally, empty cells were filled with randomly oriented Gabor elements, as described in the no path stimulus above. The average length of each backbone line segment (67 pixels) was the same as the average distance between neighbouring Gabor elements in the background. Previous studies (Field *et al.*, 1993; McIlhagga & Mullen, 1996) have shown that path detection varies inversely with the length of the backbone line segments, but in a smooth manner, so the choice of segment length was not critical.

Neither the local nor the global element density served as a cue to detection of path from no-path stimuli. The average distance from an element to its neighbour was no different for path and no-path stimuli. Secondly, the total number of empty cells were the same for path and no-path stimuli. If element density is not a cue then path

TABLE 1. Stimulus parameters in screen units

Stimulus parameter	Value
Gabor patch size (pixels)	37
Frequency of Gabor carrier (c/pixels)	0.05
Carrier phase	sine
Space constant of gaussian (pixels)	8.0
Element contrast (%)	90
Oriented	y
Number of path elements	8
Start index of elements that must be in centre	4
End index of elements that must be in centre	4
Radius of central region (pixels)	30
Path step size (pixels)	67
Jitter of path angle (deg)	4
Standard deviation of element positions (pixels)	0 varied in one experiment
Standard deviation of element orientations (deg)	0 varied in one experiment
Number of cells x direction (pixels)	13
Number of cells, y direction (pixels)	13
Cell size (pixels)	48
Duration (msec)	2000

detectability should be solely due to the alignment of elements in the path, since nothing else distinguishes path from no-path stimuli. McIlhagga and Mullen (1996) and Hess and Field (1995) confirmed this in control experiments where orientation of the path elements was randomized; they found that the path could not be detected, even under extended viewing conditions, regardless of the path angle α.

Apparatus and experimental procedures.

All stimuli were displayed on a Sony Trinitron monitor driven by a Sun Sparc station 2 computer, which generated stimuli on-line and controlled display and data collection. The mean luminance was 35 cd/m^2. The monitor was driven by an 8 bit D/A converter and an 8 bit frame buffer. The monitor was gamma corrected in software. The gamma corrected monitor behaved linearly when displaying high spatial frequencies (12 c/deg square wave) up to 90% contrast. The monitor was viewed in an otherwise indirectly lit room. Each experimental run consisted of a block of 50 trials in which in each presentation two images were presented (a path in a noise background and a noise background image alone) in random order. The subjects task was to indicate with a button press which image contained the path. In each run, the path angle α was set to 0, 5, 10, 20, 30, 40 deg etc. Each presentation was of 2 sec duration. Typically, each block was repeated twice to obtain at least 100 trials per path angle. The parameter values are given in screen units (Table 1) because the stimulus was kept constant on the screen and the viewing distance varied for individual subjects depending on their degree of amblyopia (see Methods).

Control experiments

In a number of control experiments we varied different parameters of our stimulus to evaluate its effect on amblyopic performance. This included the exposure duration which had an abrupt onset and offset, the number of path elements, the element contrast, the accuracy with which path elements were positioned on their invisible backbones and the accuracy with which the element orientation was aligned along its invisible backbone. In the latter two cases, the random variable had a Gaussian distribution with variable σ (see Figs 3 and 4).

Positional uncertainty

We measured the positional uncertainty of the amblyopic eye using a 2AFC discrimination task between a path composed of accurately positioned elements (a pedestal of zero uncertainty) and an identical path composed of elements aligned along the path with a variable amount of positional uncertainty (two-dimensional Gaussian distributed). For these measurements there were no background elements (just the path elements in isolation on a mean luminance background). A staircase procedure (200 trials) was used to collect psychometric data in the critical range and parameters estimated by fitting a Weibull function to the psychometric data. This function had the form

$$p(x) = 1 - 0.5 \times \exp\left(-\left[\frac{\xi}{\psi}\right]^{\beta}\right) \qquad (2)$$

where $p(x)$ is the probability of correctly discriminating between the two paths at a jitter variance of x. c represents the threshold and b the slope of the psychometric function. Unequal trials were handled by the fitting procedure which used maximum likelihood.

From this determination we obtained the delta uncertainty for one of a number of different path angles for each subject. To determine the level of *intrinsic uncertainty* (within the amblyopic visual system) we reversed the above procedure for the normal fellow eye. This time the increment was held fixed at the level previously determined for the fellow amblyopic eye and the pedestal uncertainty was adjusted in the manner described above. The threshold which was derived in a manner identical to that described above represented the internal pedestal of uncertainty in the amblyopic eye which corresponded to the previously determined incremental sensitivity of the amblyopic eye. We are assuming that the function describing positional uncertainty/pedestal uncertainty for the amblyopic eye is merely a laterally shifted version of that for the normal eye. In other words, external and internal uncertainty are additive [for support see Hess & Watt (1990) for normal vision and Watt & Hess (1987) for amblyopic vision]. We undertook this determination for at least three different path angles for each amblyope.

This approach is best illustrated by example. Assume the amblyopic condition introduces an intrinsic jitter in the encoded position of each path element. That is, the difference between the true position of the element and its encoded position is a Gaussian random variable with a variance of A. Now if we ask the amblyopic eye to

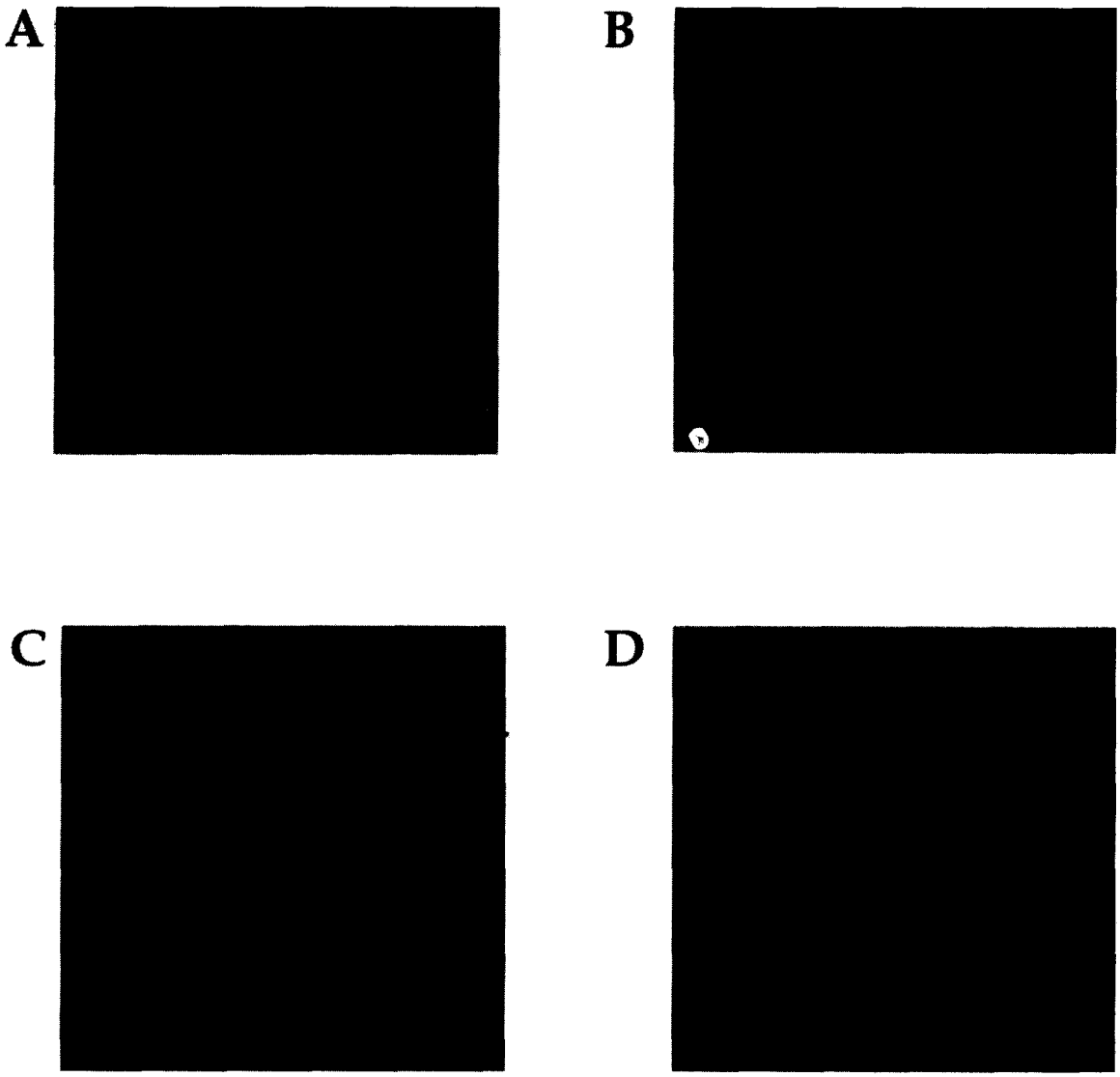

FIGURE 4. Examples of paths all of zero path angle with varying amounts of Gaussian distributed jitter added to the path element position [(A) $\sigma = 0$; (B) $\sigma = 5$ pixels; (C) $\sigma = 10$ pixels; (D) $\sigma = 20$ pixels].

discriminate between an unjittered path and one with a jitter (of variance S) then, internally, the amblyopic eye is really discriminating between jitters of A and $A + S$, since intrinsic jitter A must be added to both stimuli. Suppose the amblyopic eye attains 75% correct at a stimulus jitter of S_A. We can simulate the amblyopic condition "in the fixing eye" by doing jitter discrimination between a pedestal jitter P and a test jitter $P + S$. Suppose that the fixing eye attains 75% correct at S_G. Now find the specific pedestal jitter P^* that makes $S_G = S_A$. When this happens we must have $P^* = A$, so P^* is the intrinsic jitter in the amblyopic eye.

Its is worth emphasizing that this argument is not circular i.e. the pedestal jitter measured in the isolated path case will not inevitably produce the same performance when the path is embedded in the background. The latter case involves *detection* of the path in noise, the former *discrimination* of path regularity without noise.

Acuity measurements

We determined the grating acuity for each subject's amblyopic eye using a 2AFC task in which the subject had to choose which of two stimuli were vertically oriented. The stimuli comprised a field of randomly positioned Gabor elements whose carriers were either vertically or horizontally oriented. The screen parameters of these Gabors were identical to those used in subsequent path experiments. Viewing distance was varied until this discrimination fell to chance. A viewing distance which corresponded to one third this distance was chosen for each subject to ensure that the elements fell within their restricted spatial passband. The normal eye of each amblyope was tested at this same distance. In practice the viewing distances varied from 50 cm to 2 m. In scaling path stimuli of this kind one need to be mindful of the fact that larger stimulus fields invade more eccentric areas which may introduce an added difficulty into the task because paths falling in the periphery of the

display may not be detected within a short presentation time.

Special features

To overcome this we introduced two features into the stimulus. The first was the constraint that the central element of the path had to fall within a defined central zone which was set to a radius of 30 pixels. This ensured that paths restricted to the peripheral regions of the display were not displayed. Secondly, we set the exposure duration to 2 sec where as previously we had used 200 msec for normal vision. This ensured that there was plenty of time for an eye movement by the amblyopic eye should that be necessary. Our previous results had shown that there was only a very slight improvement in performance between exposure durations of 50 msec and 2 sec.

Clinical details

Table 1 lists the clinical details of our group of 11 strabismic amblyopes. They all have had previous experience in visual psychophysics and were given practice sessions prior to data collection. Each subject was tested on multiple occasions to check on reliability.

RESULTS

In pilot experiments on a subset of the amblyopic subjects we set out to ensure that their amblyopic performance in a contour integration task was not disadvantaged by our initial choice of stimulus parameters. We measured the acuity (see Table 1) for the stimuli that we intended to use in the contour integration task and tested at a scale (by changing viewing distance) a factor of three lower than this. The normal eye was tested at this same scale so that the stimulus conditions would be comparable. The contrast of the micropatterns was set to 90% so that they would be of comparable visibility for the normal and fellow amblyopic eye (Hess & Bradley, 1980). The duration of presentation was set to be long (2 sec) so that, should the amblyopic visual system, for one reason or another need more processing time, it would not be disadvantaged by a arbitrarily brief presentation. The middle element of the path was constrained to go through a central circular region whose radius was 30 pixels. This ensured that, for severe amblyopes who had to work at short viewing distances, paths would not be displayed in peripheral regions where attention was not directed.

Figures 5 and 6 display results for eleven amblyopes in which we compare the performance of their fixing (unfilled symbols) and fellow amblyopic (filled symbols) eyes as a function of path angle. Each amblyopic eye was tested at a scale a factor of two lower than the acuity limit for these stimuli. Each datum is the result of 100 forced choice trials. The normal eye was tested at this same scale. In all cases performance was reduced for the amblyopic eye. In most cases performance was reduced for straight paths (except O.A and Mar.S) as well as curved paths.

In a subsequent series of experiments we sought the reason for this reduced performance. Our first thought was in terms of contrast since it is known that contrast sensitivity is reduced in amblyopia. Two factors made this a less likely explanation. Our stimuli were of high contrast (90%) and previous results suggested that path detection saturates at about 20% contrast for normal observers (Field *et al.*, unpublished; McIlhagga & Mullen, 1996). Nevertheless, Fig. 7 shows results for six of our subjects in which we compare, for one representative path angle, path detection for the fixing and fellow amblyopic eye at two different contrast levels. In all cases contrast changes within this range affect fixing and amblyopic performance equally. Thus reduced visibility of the elements cannot be the reason for the reduced performance of amblyopic eyes in this contour integration task.

We next wondered whether our initial choice of a path length of 8 elements might have disadvantaged the amblyopic visual system. This would be expected if the normal eye can integrate information along longer paths than can the amblyopic eye. To assess this we varied the number of elements comprising the path. These results are shown in Fig. 8 where performance for a representative path angle is compared for the fixing and fellow amblyopic eye of three observers. Performance is seen to improve for both the fixing and fellow amblyopic eye as the number of elements comprising the path and hence its length changes. This is however no hint of any differential effect, hence it is not a likely candidate to explain the loss of performance in Figs 5 and 6.

Another possibility is that the amblyopic visual system may have defective orientation discrimination and that since orientation is the key linking feature for these paths, performance is reduced. One previous report does suggest that strabismic amblyopes are defective at least for narrowband stimuli of high spatial frequency (Skottun *et al.*, 1986). To assess this we introduced orientation-based noise into the stimuli by allowing the element orientation about the prescribed path to vary according to a Gaussian distribution. We reasoned along the lines proposed by Pelli (1980) for luminance noise, that if this is a satisfactory explanation then there should be a raised level of *intrinsic orientational noise* in the amblyopic visual system for path detection. By varying the amount of *stimulus orientational noise*, amblyopic performance should be further reduced only when the stimulus orientational noise equals the elevated intrinsic noise, thereafter normal and amblyopic performance should be equal as stimulus orientational noise increases. In Fig. 9, results are shown for path detection, at a representative path angle, for six of our amblyopic subjects as a function of the sigma of the Gaussian distribution which independently controlled the orientation of each element about the prescribed path. As Field *et al.* (1993) and Hess and Field (1995) have already mentioned, jittering the element angle has a profound effect on path detection. However, this effect is similar for the fixing and fellow amblyopic eyes. There is no evidence from these results

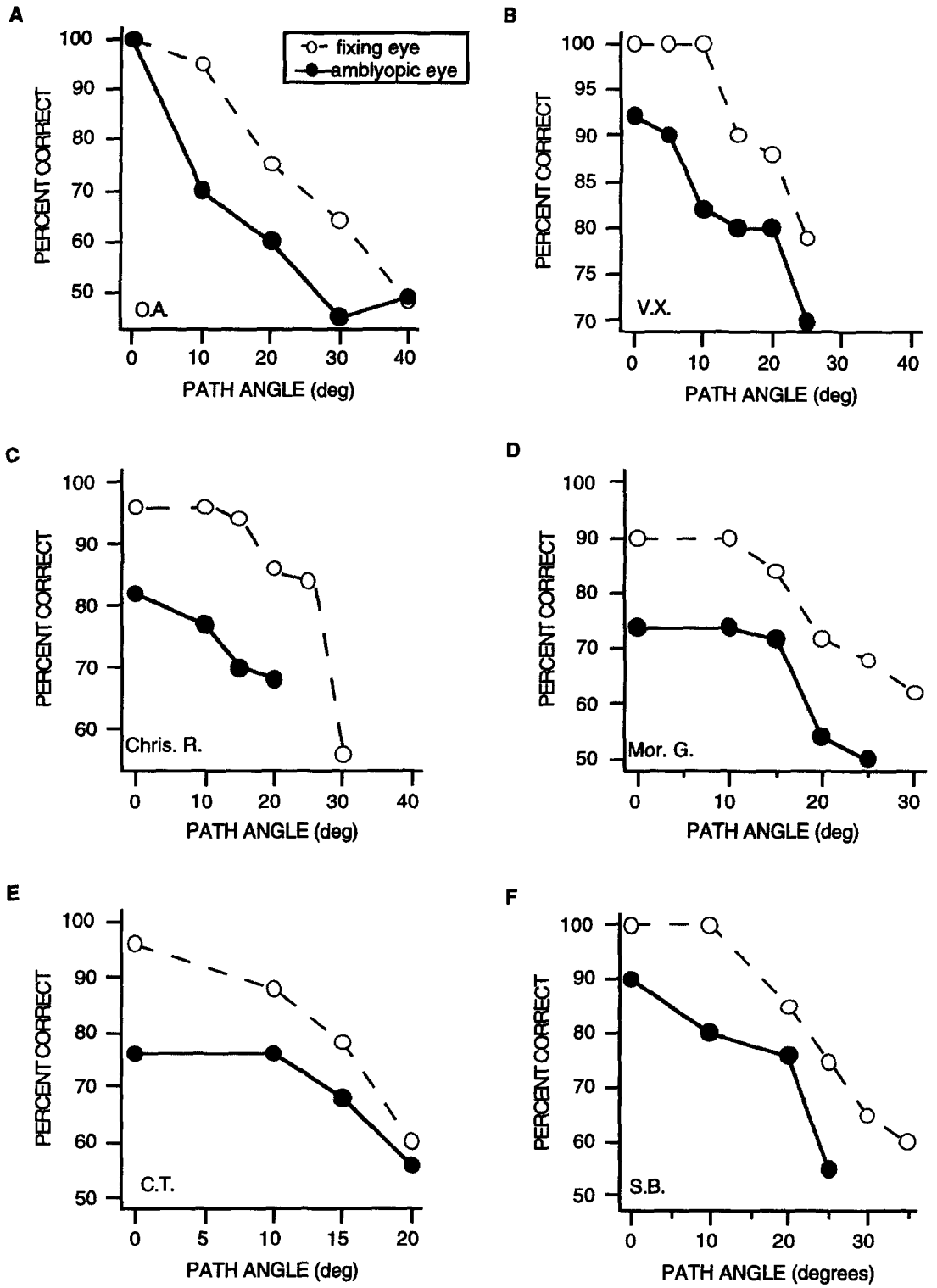

FIGURE 5. Path detection is plotted as a function of path angle for the fixing (○) and fellow amblyopic (●) eyes for six strabismic amblyopes.

that the defective performance of amblyopic eyes (Figs 5 and 6) is a consequence of a raised level of *intrinsic orientational* noise. There is no plateau in performance for the amblyopic eye at low levels of stimulus orientational noise and performance is not normal in amblyopic eyes at high levels of stimulus orientational noise.

The final and most likely possibility is that the raised level of positional uncertainty that is a characteristic of strabismic amblyopia both at (Levi & Klein, 1982, 1985, 1990) and below the acuity (Hess & Holliday, 1992; Demanins & Hess, 1996) limit is affecting performance in this task. Linking the path elements to form a perceptual contour depends on both orientation and

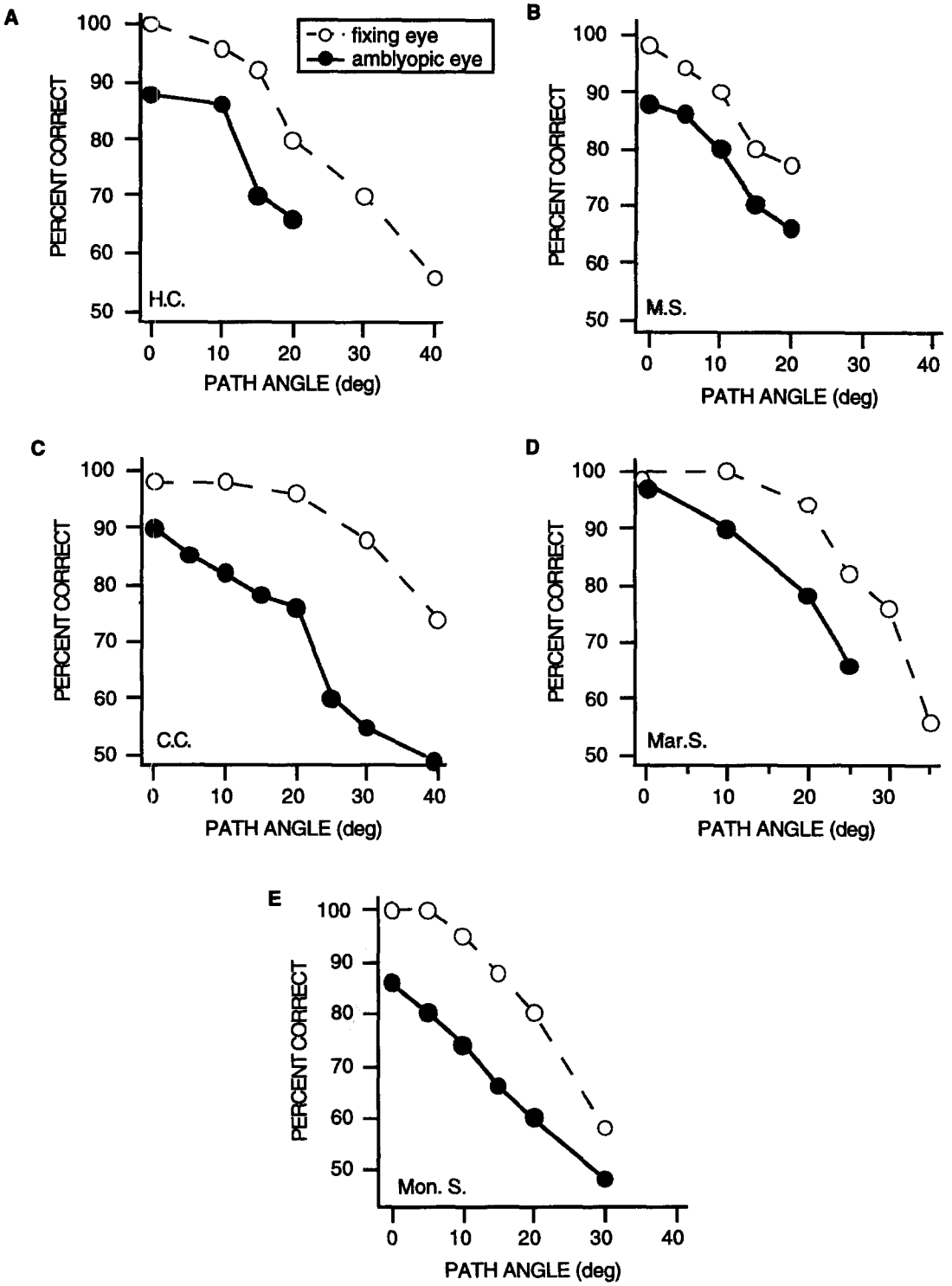

FIGURE 6. Path detection is plotted as a function of path angle for the fixing (○) and fellow amblyopic (●) eyes for five strabismic amblyopes.

distance and can be expressed in terms of a neural "association field" (Field *et al.*, 1993). Positional uncertainty must reduce performance if it is large compared with the dimensions of an "association field". To determine whether this may form the basis of a viable explanation for the reduced performance for path detection (Figs 5 and 6) we introduced a positional noise into our stimuli by independently varying the two-dimensional position of the elements comprising the path. This was done by varying the sigma of a Gaussian distribution describing each elements positional uncertainty about the prescribed path. Results are shown in Fig. 10 for path detection for six of our amblyopes in which the positional noise of the path stimuli is varied for representative path angles. Unlike the case for orientational noise, these results are suggestive of the reduced

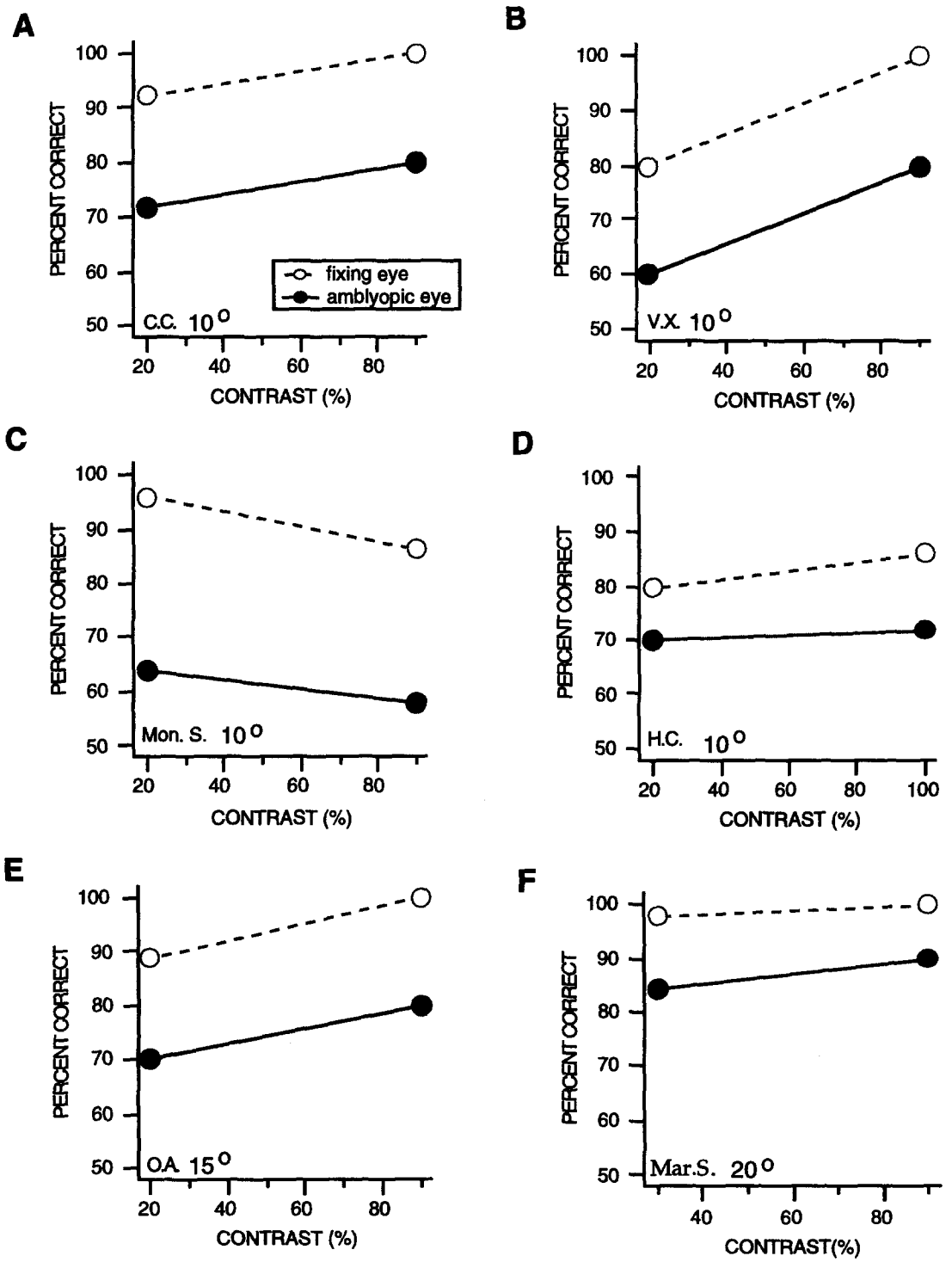

FIGURE 7. Comparison of path detection for the fixing (○) and fellow amblyopic (●) eyes of six strabismic amblyopes for two different contrast levels. Each subject was tested at one representative path angle as indicated.

performance previously seen in Figs 5 and 6 being due to a raised level of *intrinsic* positional noise (within the amblyopic visual system). The performance of the amblyopic eye is less affected by low levels of stimulus positional noise and is similar to normal at high levels of stimulus positional noise. The level of raised *intrinsic* positional uncertainty can be approximated by the level of stimulus uncertainty necessary to bring the performance of the normal and amblyopic eye together.

It would seem on the basis of the above results that a raised level of positional uncertainty within the amblyopic visual system could account for some or all of the reduced performance shown in Figs 5 and 6 where the stimulus elements were perfectly positioned along the prescribed path. If it totally accounts for the decrement in performance then we can conclude that contour integration *per se* necessary to solve this task is normal in amblyopia. If it only accounts for a part of the per-

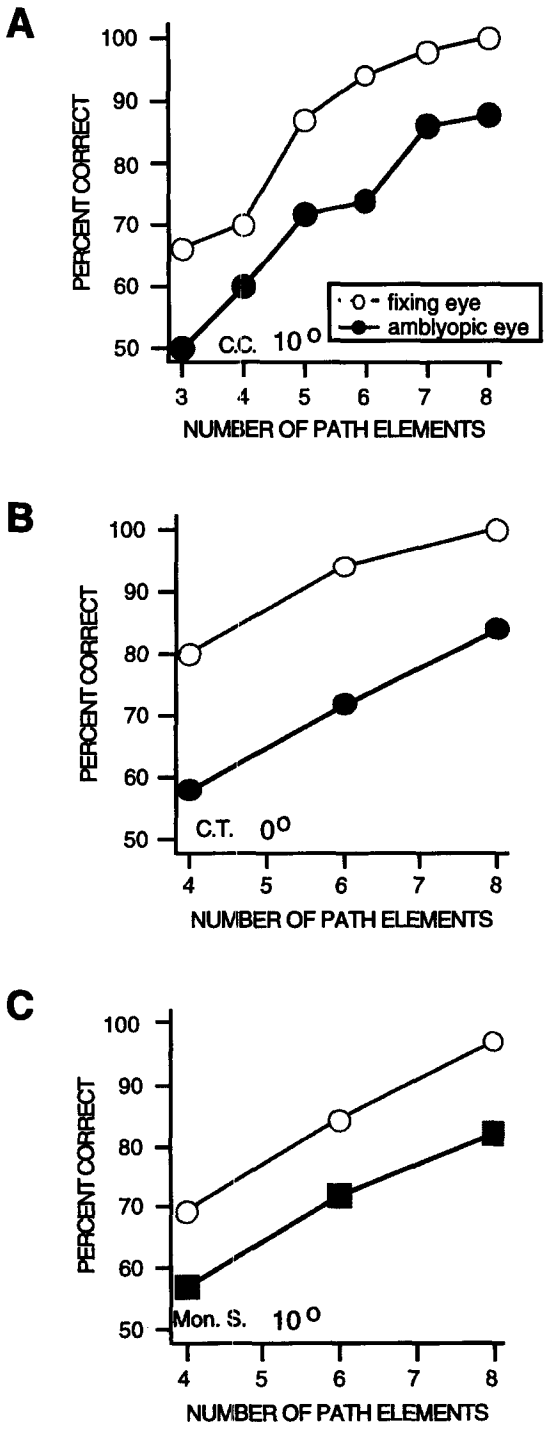

FIGURE 8. Comparison of path detection for the fixing (○) and fellow amblyopic (●) eyes of three strabismic amblyopes as a function of the number of elements comprising the path. Each subject was tested at one representative path angle as indicated.

formance decrement then a deficit more central to the disarray may be implicated. For this reason we set out to measure the *intrinsic* positional uncertainty associated with this task for each amblyope and to assess whether it represents the whole explanation for the reduced performance in this task (Figs 5 and 6).

To estimate the level of *intrinsic* positional uncertainty for this task we first measured the incremental threshold of the amblyopic eye for positional sensitivity using paths devoid from their background elements. Two presentations were given, one in which the elements were perfectly aligned along a path and another in which each element's two-dimensional position about an *identical* path was varied according to a Gaussian random variable. A staircase procedure was used to collect psychometric data and a threshold was derived by fitting an error function (see Methods). This was done for a number of different path angles for each amblyope. This gives the *incremental positional uncertainty* of the amblyopic eye corresponding to some *unknown intrinsic pedestal* within the amblyopic visual system which we wanted to derive. To estimate this *intrinsic pedestal of uncertainty* we repeated these measurements on the fellow fixing eye but this time the incremental threshold was fixed at that previously found for the fellow amblyopic eye and the pedestal was varied. This allowed us to estimate what pedestal corresponded to the incremental sensitivity of the amblyopic eye. We took this as our estimate of the *intrinsic pedestal of uncertainty* in the amblyopic visual system for that particular path angle. This procedure was repeated for a range of different path angles for each subject. These results are shown in Fig. 11(A–C). In each of these graphs, the incremental threshold for the positional uncertainty of the amblyopic eye is plotted against the subsequently measured pedestal positional uncertainty measured with the fellow fixing eye (unfilled symbols). Results are shown for three different path angles (0, 10, and 20 deg). The solid lines and filled symbols represent the increment detection function for this positional uncertainty task for a normal observer. The results are consistent with the idea that amblyopes have raised levels of positional uncertainty which elevate their incremental positional thresholds. These measures of incremental positional threshold measured with paths of zero path angle [Fig. 11(A)] comprising eight elements were highly correlated ($r = 0.80$; $0.01 < P < 0.001$) but slightly larger than those obtained from similar measurements using a three Gabor collinear alignment task [Fig. 11(D)].

Having obtained estimates of the *intrinsic positional uncertainty pedestal* in the amblyopic eyes of our subjects at a number of path angles we tested whether these levels of uncertainty could account for all of the performance decrement previously measured for path detection (Figs 5 and 6). We did this by comparing the original results for the fixing and fellow amblyopic eyes of each subject measured with perfectly aligned paths (stimulus positional uncertainty of zero as in Figs 5 and 6) with that measured for the normal fixing eye with a *stimulus* positional uncertainty equal to the *intrinsic* pedestal of uncertainty previously estimated for the fellow amblyopic eye. We reasoned that if the normal eye with a *stimulus* positional uncertainty equal to that of the fellow amblyopic eye performed comparably to that of the amblyopic eye for perfectly aligned paths (stimuli having zero positional uncertainty) then positional uncertainty is a sufficient explanation for the perfor-

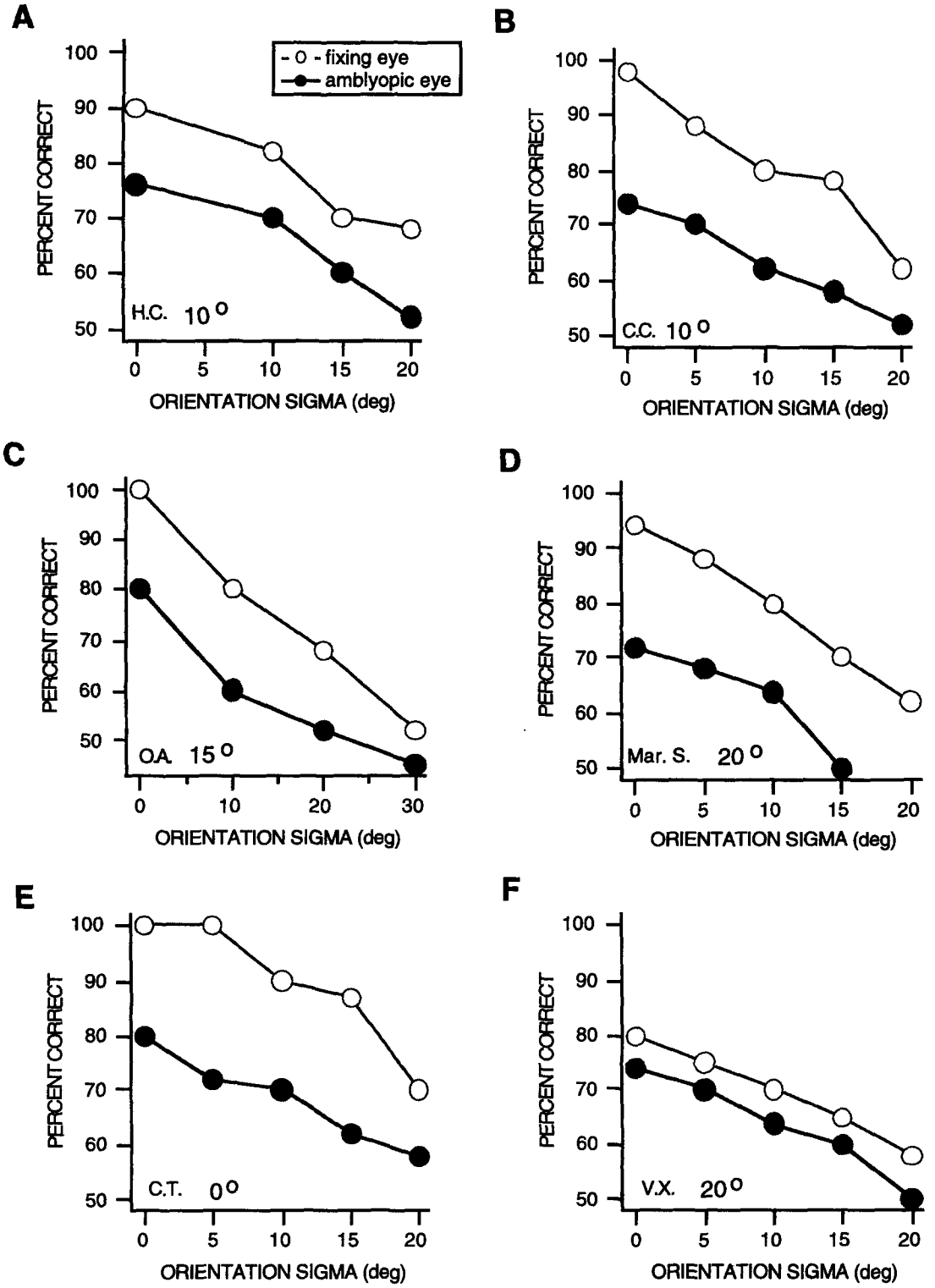

FIGURE 9. Comparison of path detection for the fixing (○) and fellow amblyopic (●) eyes of six strabismic amblyopes as a function of the extent (sigma of the Gaussian distribution) to which the orientation of individual path elements are randomized. Each subject was tested at one representative path angle.

mance decrement previously described in Figs 5 and 6. These results are shown in Figs 12 and 13 where the previous results of Figs 5 and 6 are compared with new results for the fellow fixing eye using a stimulus with a positional uncertainty equal to the intrinsic uncertainty of the amblyopic eye (unfilled bowties). In all but one case (Mon. S) an explanation based solely on a raised level of positional uncertainty adequately accounts for the previously poorer path detection exhibited by amblyopic eyes. In the one exception (Mon. S), since we could not attribute the extra performance deficit to differences in stimulus visibility, integration along the path, or a raised

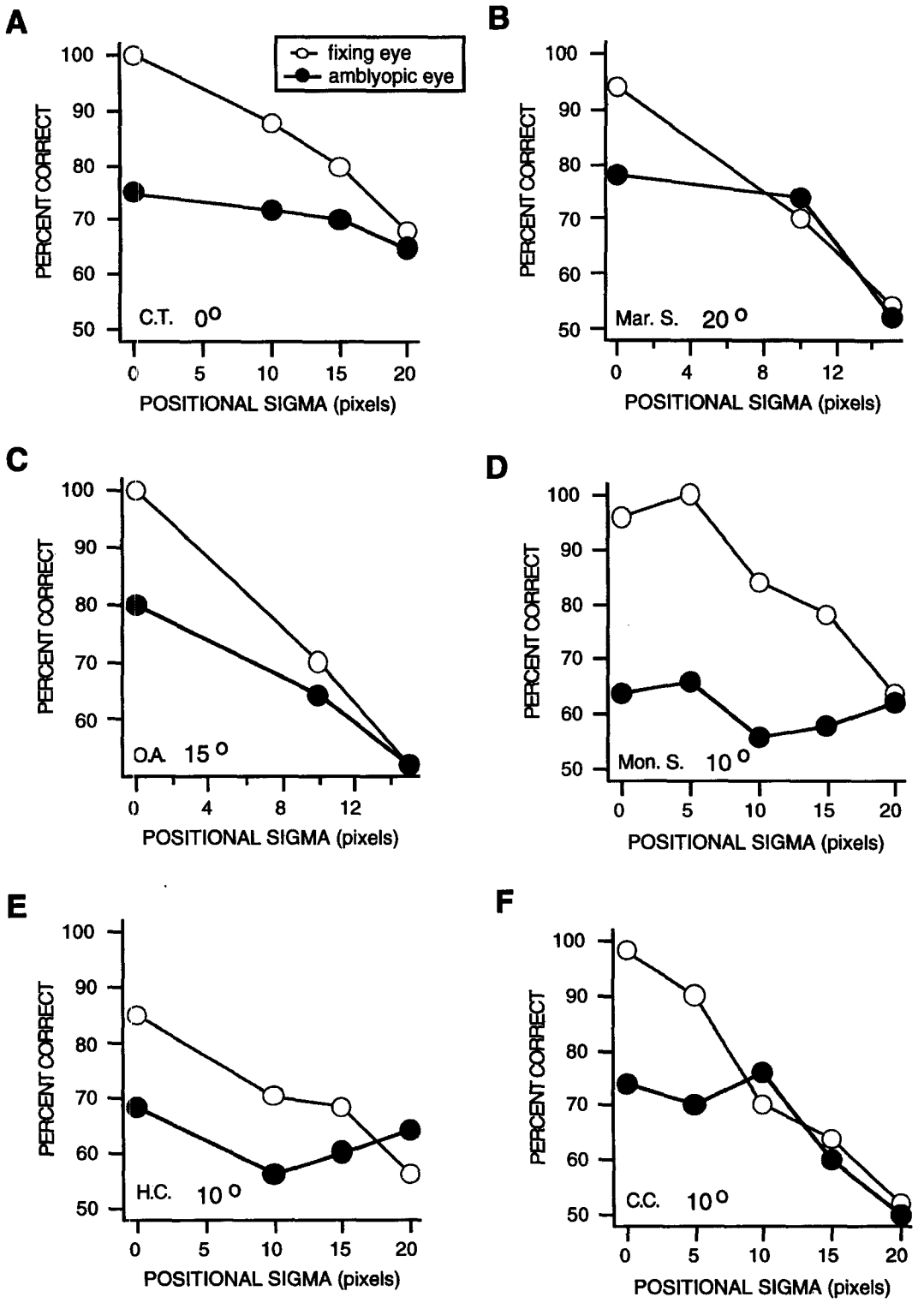

FIGURE 10. Comparison of path detection for the fixing (○) and fellow amblyopic (●) eyes of six strabismic amblyopes as a function of the extent (sigma of the Gaussian distribution) to which the two-dimensional positions of individual path elements are randomized. Each subject was tested at one representative path angle.

level of either orientational or positional noise, we are left to conclude that in some case deficits to higher integrative functions located more central to the locus of positional uncertainty exist in amblyopia.

DISCUSSION

The cortical deficit in strabismic amblyopia involves both loss of *threshold* contrast sensitivity and elevated

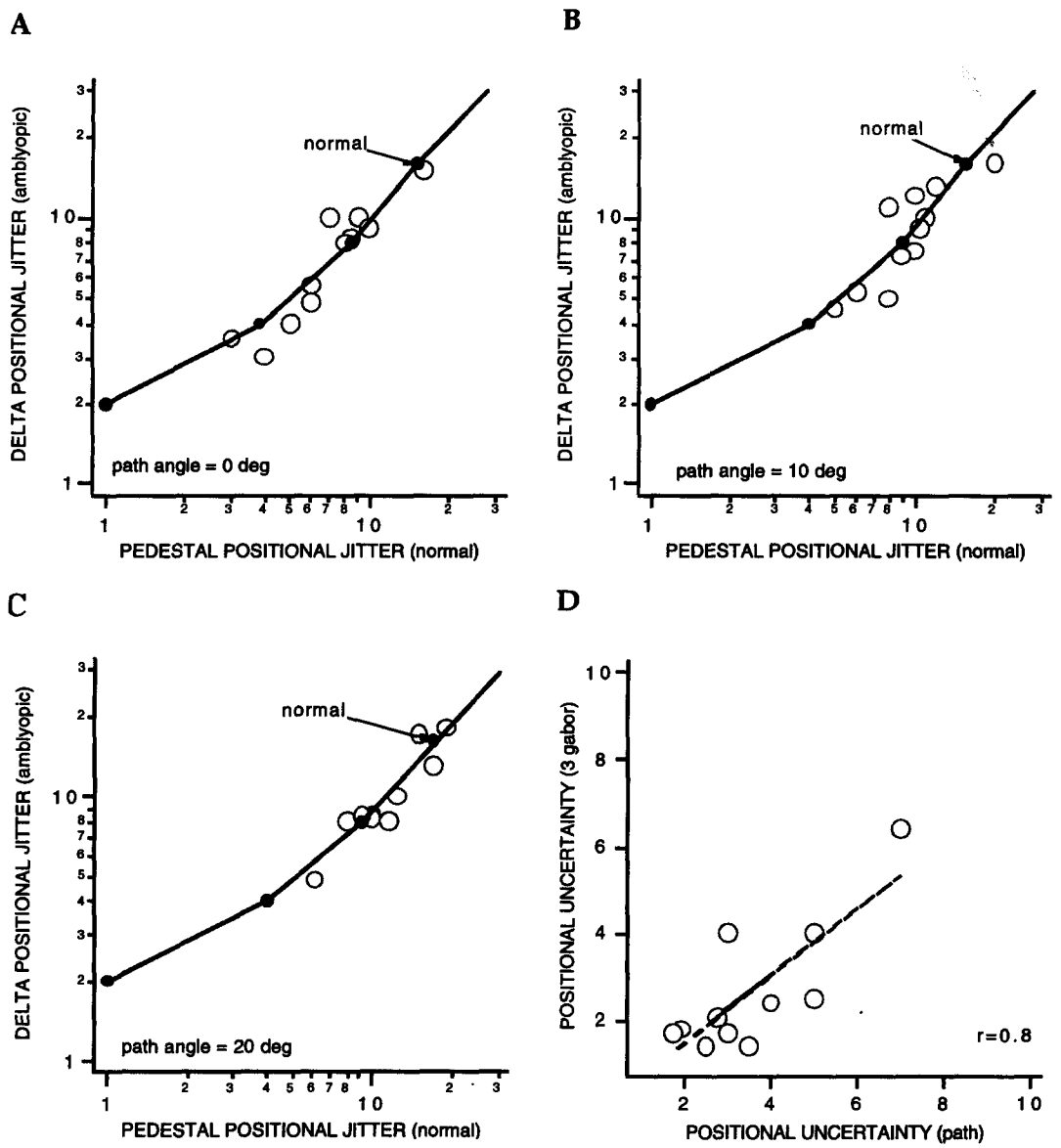

FIGURE 11. Comparison of the positional uncertainty thresholds for the amblyopic eye plotted against corresponding pedestal positional uncertainty thresholds for the fellow fixing eye (A–C). The solid line and filled symbols define the increment threshold function for positional accuracy for a normal observer. In (D), positional uncertainty for paths of zero path angle and three Gabor alignment stimuli are compared for all amblyopic eyes. The correlation coefficient is 0.8.

positional uncertainty. The former which has also been shown at the single cell level in animal models of amblyopia stems from a loss of high frequency cells and an elevation in the contrast threshold of other cells. Positional accuracy is disrupted in strabismic amblyopia at all scales (Hess & Holliday, 1992; Demanins & Hess, 1996). While much of the accuracy loss for high spatial frequency stimuli could be due to undersampling by fewer cells (Crewther & Crewther, 1990), this is a less attractive explanation for lower spatial frequency stimuli where animal models agree on there being no fewer cells driven by the amblyopic eye (Singer *et al.*, 1980; Mower *et al.*, 1982; Chino *et al.*, 1983; Freeman & Tsumoto, 1983; Crewther & Crewther, 1990; Blakemore & Vital-Durand, 1992). In agreement with this, human psychophysics also argues against any simple explanation based on undersampling for the positional deficit for stimuli well within the amblyopic passband. This is because two key predictions of any undersampling model (a correlated contrast discrimination deficit and spatial aliasing) are not part and parcel of the amblyopic syndrome (Hess & Field, 1994; Hess & Anderson, 1993).

An alternate proposal is that the elevated positional uncertainty is due to a disruption to the normal cortical topology (disarray hypothesis—Hess *et al.*, 1978; Hess, 1982) rather due to loss of cells (undersampling hypothesis—Levi & Klein, 1986). The disarray hypothesis assumes that as a consequence of strabismus early in life the projection from the two eyes differs (Hess & Field, 1994). Thus, the cortical maps from the two eyes are not in register. Consequently, learning which cortical location corresponds to which location in visual space

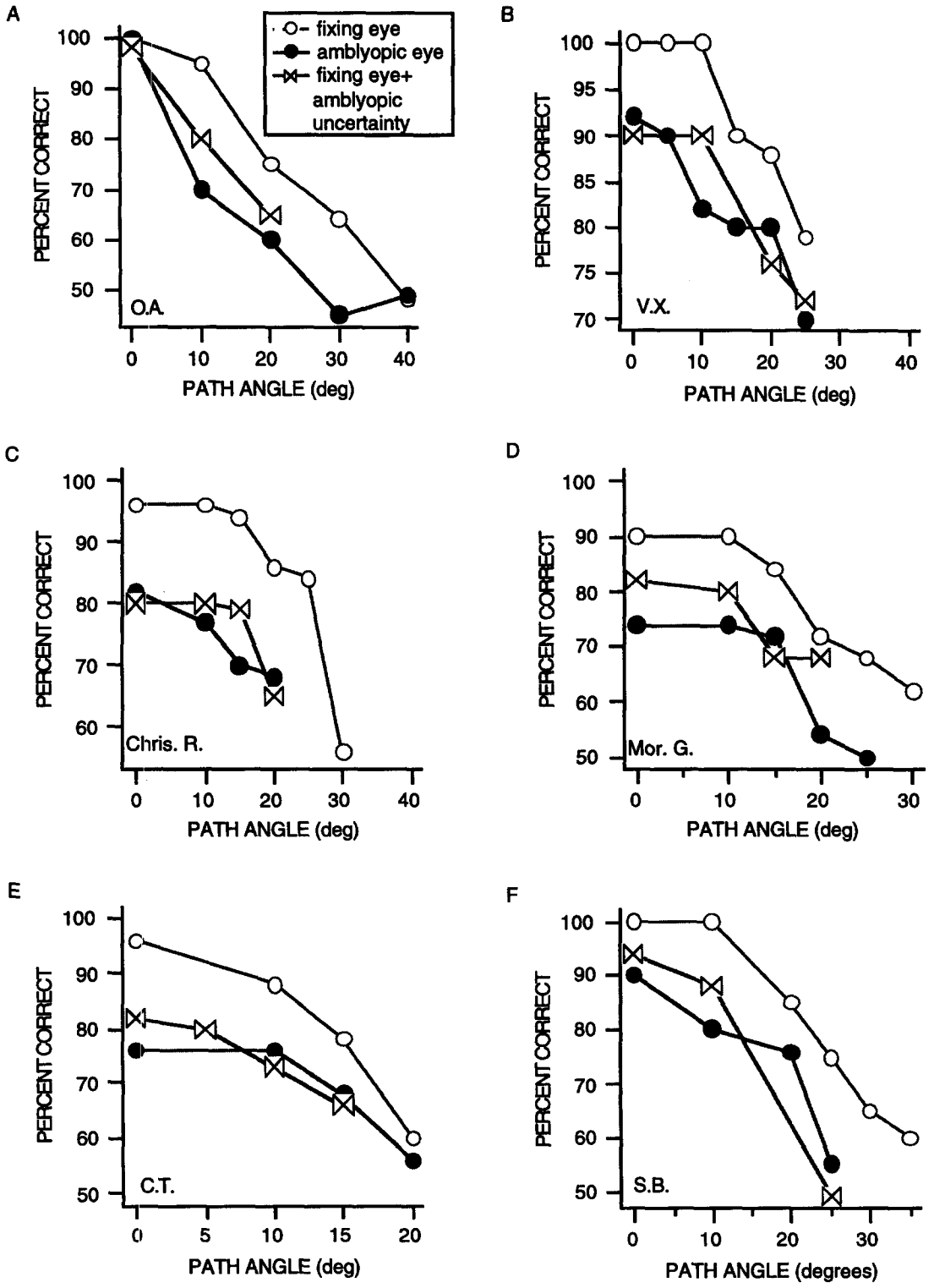

FIGURE 12. Path detection is plotted as a function of path angle for the fixing (○) and fellow amblyopic (●) eyes for six strabismic amblyopes. The open bowties are for the fixing eye with the intrinsic positional uncertainty of the fellow amblyopic eye.

can be effective for only one of the two eyes. We presume this learning or "calibration" involves intercommunication between neighbouring cells through the fine tuning of lateral connections. For example, the system could calibrate the map by using the correlations between the activity of neighbouring cells and therefore depend critically on early visual experience. However, if the two eyes have maps that are not in register, then this calibration process will be effective for only one of the two eyes. There will end up to be a map for each projection and since only one map can be correct, the other will, by definition, be incorrect or "distorted". Thus

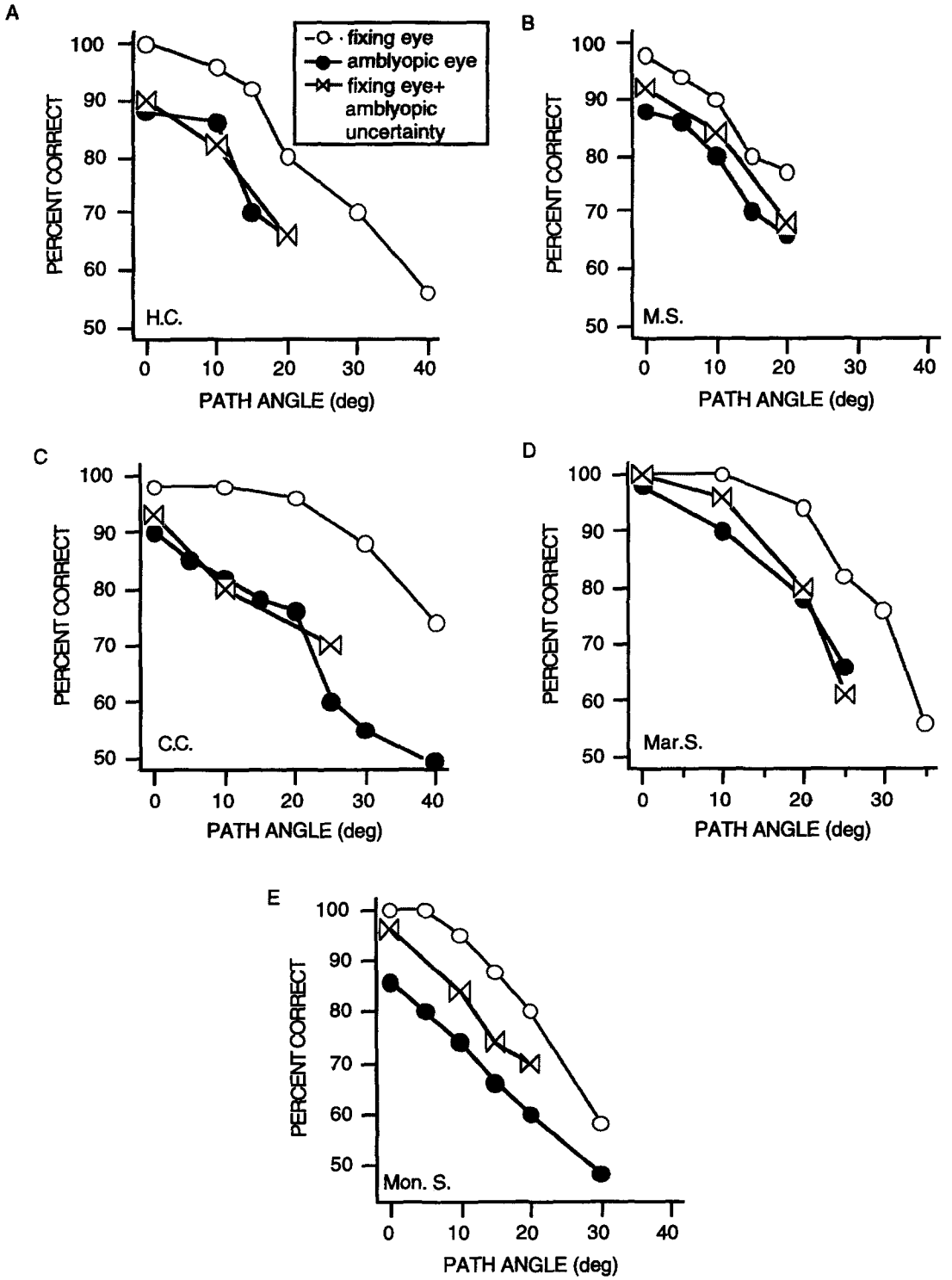

FIGURE 13. Path detection is plotted as a function of path angle for the fixing (○) and fellow amblyopic (●) eyes for five strabismic amblyopes. The open bowties are for the fixing eye with the intrinsic positional uncertainty of the fellow amblyopic eye.

the disarray hypothesis is not based solely on a passive anatomical projection abnormality but a breakdown in a dynamic process of spatial calibration which depends on lateral connections and experience.

In the present paper we use a task in which associations have to be made between neurons of specific orientations for the extraction of circular contours. We have referred to these connections between cortical orientational columns as forming an association field (Field *et al.*, 1993). The current results demonstrate that the fellow normal eye will produce equivalent errors to that of the amblyopic eye if an equivalent spatial distortion is added to the stimuli viewed by the fellow normal eye. This suggests that the integration process (e.g. the lateral

connections) in the amblyopic eye may be equivalent to the normal eye but because the connections in the amblyopic eye are between the inappropriately positioned cells, the result is a perceived distortion.

Our result is not at odds with recent reports that spatial interactions underlying contour integration are anomalous in amblyopia [Mussap & Levi (1995) for element paths exceeding eight; Polat & Sagi (1994); Polat & Norcia (1995); Kovacs *et al.* (1996)]. However, in many ways, this proposal is fundamentally equivalent to the disarray model (Hess *et al.*, 1978; Hess, 1982; Hess *et al.*, 1990; Hess & Field, 1994). If there exist connections between inappropriately positioned cells, then one could lay the blame on either the inappropriate connections or the inappropriate positions of the cells. However, what is primary in our proposal is that we propose that the fundamental source of the error is that there exists differences in the cortical maps formed from the two eyes (i.e. the relative disarray of one of the eyes is the cause of the inappropriate connections between cells).

What our results demonstrate is that an account of these positional displacements in the map is sufficient to account for the performance of amblyopic eyes. In only one of our 11 subjects was there a significant residual deficit for contour integration *per se*. Therefore, in our proposal, the proposed anomalies in the spatial interactions between neighbouring cells is due to the relative disarray found in the cortical projections of the two eyes. Any proposal that argues that the problem is ONLY a result of an error in the spatial interactions would require a theory of why such anomalous spatial interactions would occur in only one of the two eyes.

REFERENCES

Blakemore, C. & Vital-Durand, F. (1992). Different neural origins for blur amblyopia and strabismic amblyopia. *Ophthalmological and Physiological Optics, 12*, 83–90.

Chino, Y. M., Shansky, M. S., Jankowski, W. L. & Banser, E. A. (1983). Effects of rearing kittens with convergent strabismus on development of receptive field properties in striate cortical neurons. *Journal of Neurophysiology, 50*, 265–286.

Crewther, S. G. & Crewther, D. P. (1990). Neural site of strabismic amblyopia in cats, spatial frequency deficit in primary cortical neurons. *Experimental Brain Research, 79*, 615–622.

Demanins, R. & Hess, R. F. (1996). Positional loss in strabismic amblyopia: Inter-relationship of alignment thresholds, bias, spatial scale and eccentricity. *Vision Research, 36*, 2771–2794.

Field, D. J., Hayes, A. & Hess, R. F. (1993). Contour integration by the human visual system; Evidence for a local "association field". *Vision Research, 33*, 173–193.

Freeman, R. D. & Tsumoto, T. (1983). An electrophysiological comparison of convergent and divergent strabismus in the cat: Electrophysiological and visual activation of single cortical cells. *Journal of Neurophysiology, 49*, 238–253.

Hess, R. F. (1982). Developmental sensory impairment; Amblyopia or tarachopia? *Human Neurobiology, 1*, 17–29.

Hess, R. F. & Anderson, S. J. (1993). Motion sensitivity and spatial undersampling in amblyopia. *Vision Research, 33*, 881–896.

Hess, R. F. & Bradley, A. (1980). Contrast perception above threshold is only minimally impaired in human amblyopia. *Nature, 287*, 463–464.

Hess, R. F., Campbell, F. W. & Greenhalgh, T. (1978). On the nature of the neural abnormality in human amblyopia: Neural aberration and neural sensitivity loss. *Pflügers Archiv fur die gesamte Physiologie, 377*, 201–207.

Hess, R. F. & Field, D. J. (1994). Is the spatial deficit in strabismic amblyopia due to loss of cells or an uncalibrated disarray of cells?. *Vision Research, 34*, 3397–3406.

Hess, R. F. & Field, D. J. (1995). Contour integration across depth. *Vision Research, 35*, 1699–1711.

Hess, R. F., Field, D. J. & Watt, R. J. (1990). The puzzle of amblyopia. In Blakemore, C., (Ed.), *Vision coding and efficiency* (chap. 25, pp. 267–280). Cambridge: Cambridge University Press.

Hess, R. F. & Holliday, I. E. (1992). The spatial localization deficit in amblyopia. *Vision Research, 32*, 1319–1339.

Hess, R. F. & Pointer, J. S. (1985). Differences in the neural basis of human amblyopia: The distribution of the anomaly across the visual field. *Vision Research, 25*, 1577–1594.

Hess, R. F. & Watt, R. J. (1990). Regional distribution of the mechanisms that underlie spatial localization. *Vision Research, 30*, 1021–1031.

Kovacs, I. & Julesz, B. (1993). A closed curve is much more than an incomplete one: Effect of closure in completion of segmented contours. *PNAS U.S.A., 90*, 7495–7497.

Kovacs, I., Polat, U. & Norcia, A. M. (1996). Breakdown in binding mechanisms in amblyopia. *Investigative Ophthalmology & Visual Science, 37*(Suppl.), 670.

Levi, D. M. & Klein, S. A. (1982). Hyperacuity and amblyopia. *Nature, 298*, 268–270.

Levi, D. M. & Klein, S. A. (1985). Vernier acuity, crowding and amblyopia. *Vision Research, 25*, 979–991.

Levi, D. M. & Klein, S. A. (1986). Sampling in spatial vision. *Nature, 320*, 360–362.

Levi, D. M. & Klein, S. A. (1990). Equivalent intrinsic blur in amblyopia. *Vision Research, 30*, 1995–2022.

McIlhagga, W. & Mullen, K. T. (1996). Contour integration with colour and luminance contrasts. *Vision Research, 36*, 1265–1279.

Mower, G. D., Burchfiel, J. L. & Duffy, F. H. (1982). Animal studies of strabismic amblyopia: Physiological studies of visual cortex and the lateral geniculate nucleus. *Developmental Brain Research, 5*, 311–327.

Mussap, A. J. & Levi, D. M. (1995). Amblyopic deficits in the perception of second-order orientation. *Investigative Ophthalmology & Visual Science, 36*, 634.

Pelli, D. G. (1980). The quantum efficiency of vision, In Blakemore, C., (Ed.), *Vision coding and efficiency* (chap. 1, pp. 3-24). Cambridge: Cambridge University Press.

Polat, U. & Norcia, A. M. (1995). Neurophysiological evidence of long range interactions in normal and amblyopic human visual cortex. *Investigative Ophthalmology & Visual Science, 36*, 673.

Polat, U. & Sagi, D. (1994). Spatial interactions in normal and amblyopic observers: Is there a qualitative difference. *Investigative Ophthalmology & Visual Science, 35*, 1257.

Singer, W., von Grunau, M. & Rauschecker, J. (1980). Functional amblyopia in kittens with unilateral exotropia. *Experimental Brain Research, 40*, 294–304.

Skottun, B. C., Bradley, A. & Freeman, R. D. (1986). Orientation discrimination in amblyopia. *Investigative Ophthalmology & Visual Science, 27*, 532–537.

Watt, R. J. & Hess, R. F. (1987). Spatial information and uncertainty in anisometropic amblyopia. *Vision Research, 27*, 661–674.

Acknowledgements—This work was supported by a Grant (No. MT 108-18) form the Medical Research Council of Canada. We are very grateful to R. Demanins for her help in all aspects of this project and Cristyn Williams for comments on the manuscript.